JOURNAL OF GEOPHYSICAL RESEARCH, VOL. 101, NO. D1, PAGES 1931–1941, JANUARY 20, 1996

# Upper tropospheric water vapor and cirrus: Comparison of DC-8 observations, preliminary UARS microwave limb sounder measurements and meteorological analyses

Reginald E. Newell[1], Yong Zhu[1], Edward V. Browell[2], Syed Ismail[2], William G. Read[3], Joe W. Waters[3], Kenneth K. Kelly[4], and Shaw C. Liu[4]

**Abstract**. Upper tropospheric water vapor in the tropical West Pacific has been examined by three approaches that were operational during the NASA Pacific Exploratory Mission-West A (PEM-West A) in September-October 1991: direct measurement with a Lyman-α fluorescence instrument on the NASA DC-8; remote sensing by the microwave limb sounder (MLS) on the Upper Atmosphere Research Satellite (UARS); and deduction of cirrus clouds by differential absorption lidar (DIAL) flown on the DC-8 together with environmental conditions derived from meteorological analyses made by the European Centre for Medium-Range Weather Forecasts (ECMWF). Comparison between the DC-8 direct measurement and the preliminary MLS (12 cases) estimates showed fair agreement with a tendency for MLS to show an overestimate at low mixing ratio values (≤ ~200 parts per million by volume). The comparison between the DIAL and the ECMWF analyses (13 cases) showed that cirrus occurred in regions where there was rising motion and relative humidity near 100%. The DIAL observations are from much smaller spatial regions than can be resolved from the ECMWF analyses. The cirrus tops occurred below the tropopause as measured by the vertical ozone gradient in the DIAL data; no cases of tropopause penetration were observed during this season. In most cases the cirrus formed in air of low potential vorticity and relatively low ozone. At 150 and 200 hPa the center of the rising motion, as shown by the maximum in the velocity potential pattern based on the ECMWF analysis, is at about 18°N, 145°E in close correspondence to the MLS water vapor mixing ratio maximum deduced for 147 and 215 hPa.

## Introduction

As part of the NASA Global Tropospheric Experiment, the NASA DC-8 was deployed to the western Pacific region in September-October 1991 to measure atmospheric trace gases and aerosol in airstreams coming off the Asian continent and to compare their concentrations with those in relatively clean marine air entering the region from the east. This mission, known as Pacific Exploratory Mission-West A (PEM-West A), laid strong emphasis on the ozone and sulphur cycles and involved other trace gases which play a role in these cycles such as carbon monoxide, nitric oxide, and water vapor. Upper tropospheric water vapor was measured on the DC-8 with a Lyman-α resonance fluorescence hygrometer [*Kley and Stone*, 1978] modified from the one used in the high-altitude aircraft (ER-2) mission carried out over Darwin in January and February 1987 [*Kelly et al.*, 1993]. At altitudes below about 5 km the Lyman-α instrument saturates and two standard frostpoint hygrometers were used to measure water vapor; these lower troposphere measurements are not considered in this paper. Preliminary estimates of upper tropospheric water vapor are also available from the Upper Atmosphere Research Satellite (UARS) microwave limb sounder (MLS) which became operational about one week after the September 12, 1991, launch of UARS. *Read et al.* [1995] discuss how upper troposphere water is obtained from MLS, *Waters* [1993] gives the MLS measurement principles, and *Barath et al.* [1993] describe the UARS instrument. MLS water vapor results used here are 2.5 to 3-km-thick layer averages, for layers centered at 215 and 316 hPa (relatively near the pressure levels flown by the DC-8 during PEM-West A). It should be emphasized that the current MLS upper tropospheric water vapor results are preliminary and obtained from a relatively unsophisticated retrieval algorithm which yields a precision estimate of about 30%; further work is under way by the MLS team to improve their quality and confidence.

[1]Massachusetts Institute of Technology, Cambridge.
[2]NASA Langley Research Center, Hampton, Virginia.
[3]Jet Propulsion Laboratory, California Institute of Technology, Pasadena.
[4]NOAA, Boulder, Colorado.



Paper number 95JD01373.
0148-0227/96/95JD-01373$05.00

The DC-8 also measured aerosols and ozone with an airborne differential absorption lidar (DIAL), with nadir- and zenith-pointing instruments for obtaining a two dimensional cross section of aerosols and ozone from near the surface (or cloud top if cloud was present below the aircraft) to well above the tropopause along the flight track [see *Browell et al.*, this issue]. Most of the time the aerosols seen above the DC-8 when it was flying at 8 km or higher had the characteristics of cirrus clouds: their scattering ratio, relative to molecular scattering, was large, and the wavelength dependence of the scattering was small. In the vicinity of this cloud the water vapor mixing ratio would be expected to be close to that corresponding to saturation over ice at the appropriate temperature and pressure. Thus if the latter two variables could be obtained at the cirrus altitude, then the corresponding water vapor may also be compared with that measured by the MLS.

During PEM-West A, extensive use of the meteorological analyses drawn up by the European Centre for Medium-Range Weather Forecasts (ECMWF) for their numerical forecast model was made as part of the flight planning process; after the mission the full set of grid point data on wind velocity, vertical motion, geopotential, temperature, and relative humidity were provided as a function of pressure. Relatively little data on upper tropospheric humidity is incorporated into these analyses, although the situation has improved since June 1992 in regions north of 20°N [see *Eyre et al.*, 1993]. However, temperature is well analyzed and, in principle, it is therefore possible to use ECMWF temperature data and assume saturation at the DIAL-observed cirrus level to deduce water vapor mixing ratios; but the vertical extent of the cirrus precludes a direct comparison with the MLS observations. However, the DIAL-observed cirrus may be

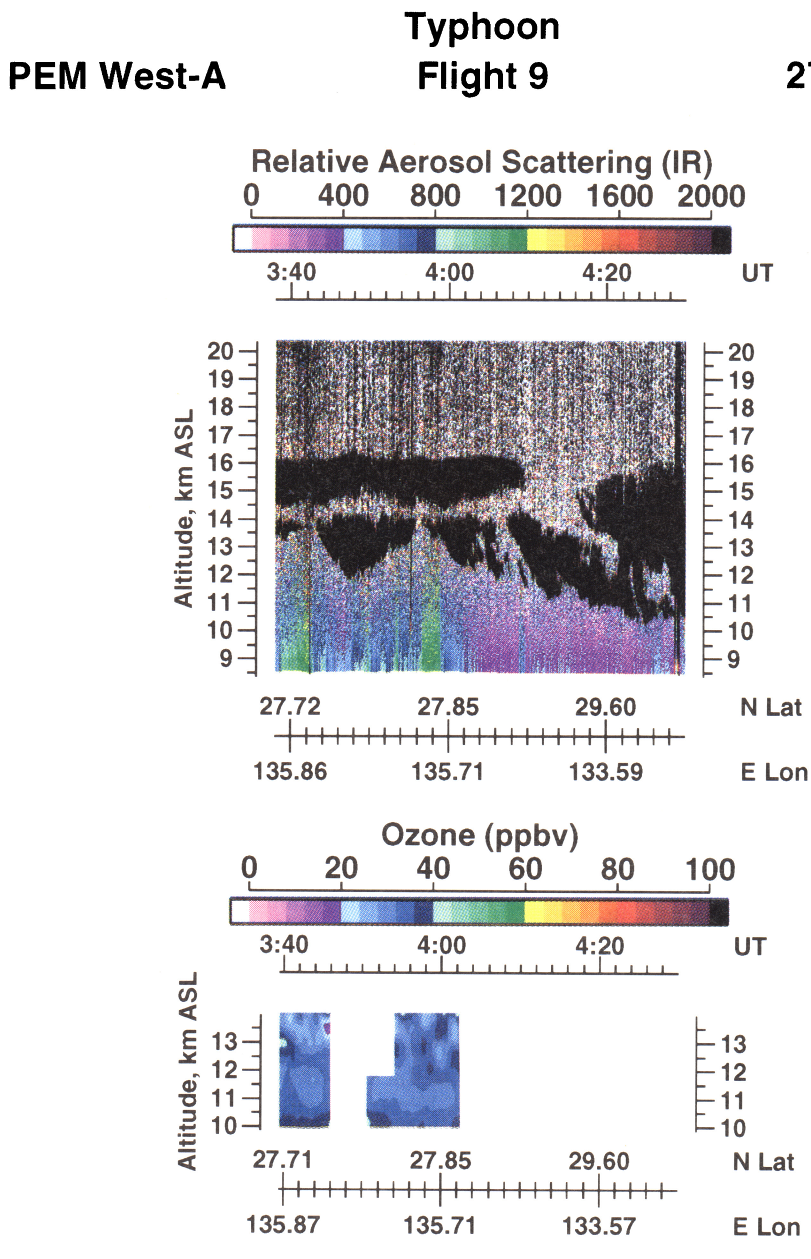


**Plate 1.** DIAL cross section along DC-8 flight track of aerosol and ozone for September 27, 1991.

**Table 1.** Comparison of Measurements of Water Vapor With Lyman-α Instrument on DC-8 With Microwave Limb Sounder on UARS

| | | | DC-8 | | | | | | | | | | MLS | | |
|---|---|---|---|---|---|---|---|---|---|---|---|---|---|---|---|
| PEM Mission | UARS Day | 1991 | Sampling Period, UT | | Lat N | Long E | Aircraft in Cloud | p hPa | q ppmv | s(q), ppmv | Observation | ECMWF ω $10^{-2}$ Pa $s^{-1}$ | q at 215 hPa, ppmv | q at 316 hPa, ppmv | Adopted q, ppmv |
| 6 | 11 | Sept. 22 | 0834 | 0842 | 30°4'<br>30°2' | 145°51'<br>144°32' | no | 325 | 159 | 3.0 | 291 | 10 | 114 | 255 | 265 |
| 10 | 20 | Oct. 1 | 0400 | 0426 | 28°27'<br>26°12' | 140°17'<br>137°40' | no | 327 | 205 | 0.03 | 1552 | 10 | 100 | 200 | 209 |
| 12 | 23 | Oct. 4 | 0625 | 0636 | 24°43'<br>23°26' | 122°15'<br>121°44' | no | 260 | 487 | 0.1 | 651 | 0 | 114 | 280 | 195 |
| 12 | 23 | Oct. 4 | 0912 | 0920 | 22°91<br>22°20' | 118°38'<br>117°31' | haze | 326 | 653 | 4.0 | 459 | -10 | 114 | 280 | 293 |
| 13 | 25 | Oct. 6 | 0510 | 0530 | 28°5'<br>26°20' | 123°49'<br>122°14' | no | 326 | 257 | 0.7 | 1200 | 5 | 90 | 265 | 279 |
| 14 | 27 | Oct. 8 | 0551 | 0600 | 14°40'<br>13°38' | 132°6'<br>131°25' | no | 194 | 126 | 1.0 | 540 | 0 | 210 | 430 | 150 |
| 15 | 30 | Oct. 11 | 0616 | 0620 | 8°35'<br>8°52' | 150°57'<br>150°32' | no | 225 | 140 | 0.3 | 240 | 0 | 218 | 460 | 245 |
| 16 | 32 | Oct. 13 | 0200 | 0230 | 8°23'<br>6°47' | 136°14'<br>132°39' | no | 326 | 479 | 1.3 | 1792 | 5 | 200 | 440 | 459 |
| 16 | 32 | Oct. 13 | 0728 | 0742 | 12°7'<br>12°56' | 142°25'<br>143°49' | haze | 215 | 83 | 0.1 | 840 | -10 | 191 | 400 | 191 |
| 17 | 33 | Oct. 14 | 2040 | 2054 | 15°0'<br>15°0' | 140°17'<br>138°28' | no | 326 | 594 | 1.4 | 840 | 10 | 206 | 358 | 370 |
| 18 | 37 | Oct. 18 | 0010 | 0012 | 12°53'<br>12°49' | 147°31'<br>147°45' | haze | 259 | 131 | 0.9 | 96 | 2 | 180 | 300 | 240 |
| 19 | 37 | Oct. 18 | 2230 | 2315 | 18°50'<br>19°29' | 169°67'<br>175°46' | no | 259 | 171 | 1.3 | 2689 | 0 | 80 | 182 | 130 |

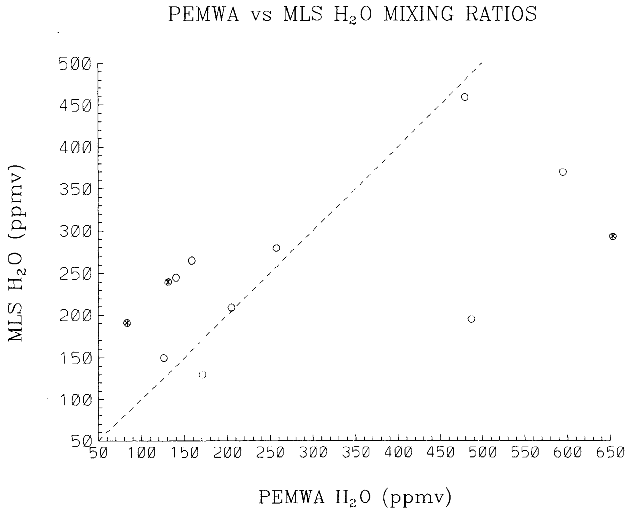


**Figure 1.** Comparison of water vapor measured by Lyman-$\alpha$ instrument on DC-8 with that deduced from microwave limb sounder (MLS) in same region. Units, parts per million by volume. Points marked with asterisk correspond to haze cases in Table 1.

compared with ECMWF rising motion and 100% relative humidity regions, recognizing that the DC-8 gives data in much smaller spatial regions than those resolved in the ECMWF analysis.

## DC-8 Water Vapor Versus MLS Water Vapor

There were 12 occasions when the DC-8 measured water vapor in the upper troposphere, and concomitant MLS measurements at 215 and 316 hPa were available. These DC-8 measurements were outside cloud, the presence of which influences the Lyman-$\alpha$ instrument. These data are summarized in Table 1. The sampling periods and latitudes and longitudes at the beginning and end of the sampling periods are noted, as well as the aircraft pressure level. The instrument samples every second, and the large number of independent samples used accounts for the small standard deviations associated with the mixing ratio values. On three occasions haze was present, but this does not necessarily influence the instrument unless the haze contains cirrus cloud particles.

The along-orbit MLS water vapor mass mixing ratio values (q) were plotted and hand-drawn contours were used

**Table 2.** Comparison of DIAL Aerosol (Cirrus) Layers and Ozone With ECMWF Relative Humidity, Vertical Motion, and Potential Vorticity

| | | Selected Point for Comparison | | DIAL Aerosol | | 90% RH Layer | | ECMWF | | | |
|---|---|---|---|---|---|---|---|---|---|---|---|
| Mission, Date | Image No. | Lat. | Long. | Base, km | Top, km | Base, km | Top, km | $\omega$ at Layer Center $10^{-2}$ Pa $s^{-1}$ | PV at Center $10^{-7}$ $\frac{\deg m^2}{kg\ s^{-1}}$ | DIAL $O_3$ at Center, ppbv | Aerosol Top Near Tropopause? |
| 6, Sept. 22 | 20 | 27.0°N | 145.0°E | 10.0 | 12.0 | 10.2 | 11.8 | -10 | 7 | <40 | yes |
| 7, Sept. 24 | 26 | 35.0°N | 146.0°E | 12.0 | 12.7 | 11.9 | 12.3 | -4 | 4 | ~60* | yes |
| 8, Sept. 25 | 40 | 32.9°N | 142.5°E | 10.0 | 13.0 | 10.5 | 13.5 | -20 | 1 | ~25 | yes |
| 9, Sept. 27 | 44 | 27.7°N | 135.8°E | 12.0 | 16.0 | 14.0 | 15.2 | -3 | 3 | ~20 | yes |
| 10, Oct. 1 | 50 | 19.1°N | 125.5°E | 11.5 | 16.0 | 13.8 | 16.0 | -2 | 1 | ~25 | yes |
| 11, Oct. 2 | 52 | 20.8°N | 120.8°E | 9.8 | 15.5 | 10.5 | 13.6 | -16 | 1 | <40 | no, 1 km below |
| 12, Oct. 4 | 58 | 21.8°N | 121.0°E | 10.5 | 13.0 | 11.8 | 13.8 | +14 | 2 | <40 | yes |
| 14, Oct. 8 | 70 | 18.3°N | 124.0°E | 10.0 | 15.8 | 10.2 | 14.8 | -4 | <1 | ~10 | yes |
| 16, Oct. 13 | 86 | 6.9°N | 134.0°E | 15.7 | 17.0 | 13.3 | 15.8 | +1 | 10 | <100† | no |
| 17, Oct. 14 | 96 | 15.0°N | 140.3°E | 11.5 | 16.0 | 11.0 | 13.0 | -2 | 2 | ~35 | yes |
| 18, Oct. 18 | 101 | 12.8°N | 153.0°E | 12.5 | 15.2 | 11.5 | 14.7 | -4 | 3 | - | - |
| 19, Oct. 19 | 106 | 19.3°N | 173.7°E | 13.0 | 15.5 | 13.2 | 15.5 | -2.5 | 3 | 42 | yes |
| 20, Oct. 20 | 112 | 19.6°N | 155.8°W | 13.0 | 15.0 | 11.0 | 13.0 | -2 | ~3 | ~40 | yes |

ECMWF, European Center for Medium-Range Weather Forecasts; DIAL, differential absorption lidar.
*This value is elevated because it is in vicinity of a stratospheric intrusion. There is also a resolution problem.
†The DIAL measurement of ozone did not resolve this thin aerosol layer.

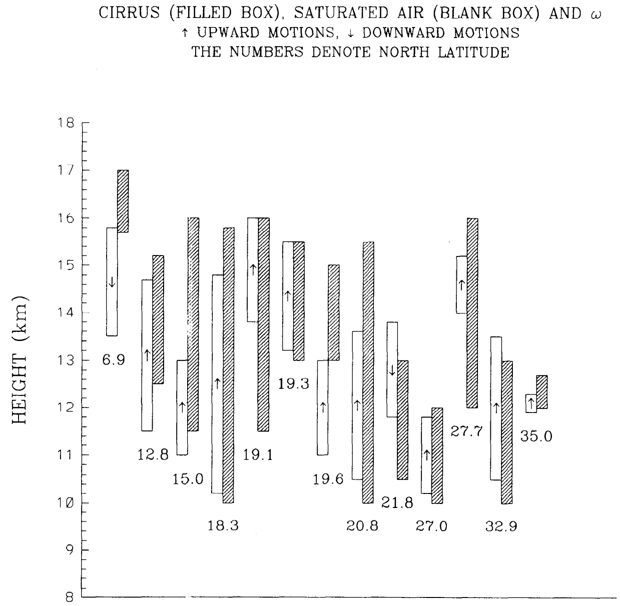


**Figure 2**. Comparison of cirrus altitude range measured by differential absorption lidar (DIAL) with European Center for Medium-Range Weather Forecasts (ECMWF) vertical motion (ω) and vertical extent of layer with relative humidity greater than 90%.

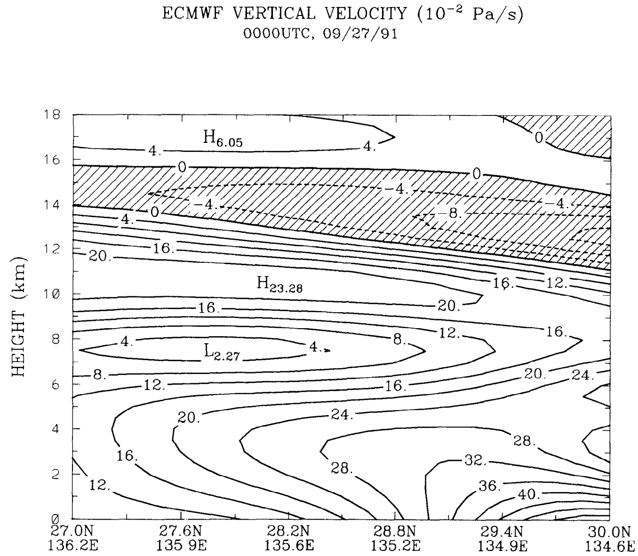


**Figure 3b**. Cross section of vertical motion in $10^{-2}$ Pa $s^{-1}$ from ECMWF data for September 27, 1991. Rising motion shaded.

to estimate the patterns; these were compared with ECMWF vertical motion patterns to assist in deciding whether patterns of water vapor were associated with atmospheric features. The vertical motion at the aircraft position is given in the central column of Table 1. Except for two cases when haze was reported, large-scale sinking motion prevailed. MLS values are available at 147, 215, and 316 hPa (about 14.3, 12, and 9 km, respectively). In most cases the DC-8 flew close to one of the two latter levels, but even when it did not, the water vapor mixing ratio for comparison was obtained from a logarithmic pressure interpolation from the MLS data to the DC-8 flight altitude. The adopted mixing ratio for comparison is given in the last column. The data sets are compared in Figure 1. The maximum value of q of 653 parts per million per volume (ppmv) is associated with haze, and in this case the Lyman-α instrument may read high because of entrained cirrus particles; the DC-8 value of 487 ppmv occurred when the plane had just left a cloudy region. Thus the October 4 data, while plotted in Figure 1, are excluded from the comparison. The October 14 value of 594 ppmv for the DC-8 occurred immediately after a 30-min run in the tropical boundary layer and could also be suspect. In two other cases (marked on Figure 1), haze was reported from perusal of the aircraft videos. Excluding

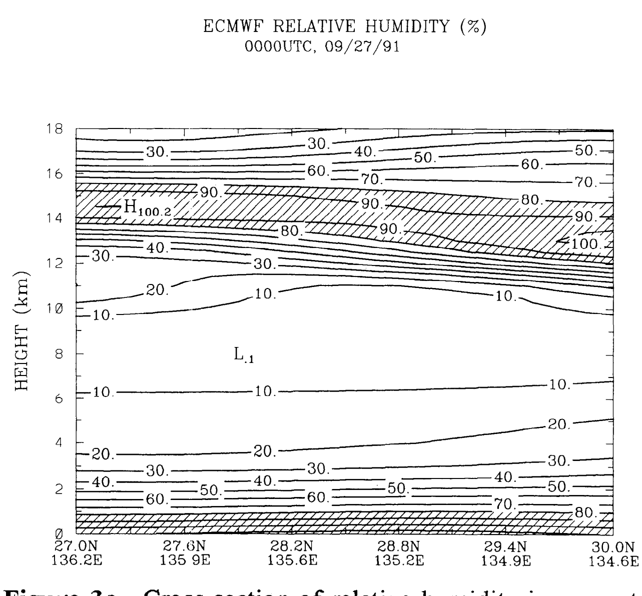


**Figure 3a**. Cross section of relative humidity in percent drawn up from ECMWF grid point data for September 27, 1991. Values >80% shaded.

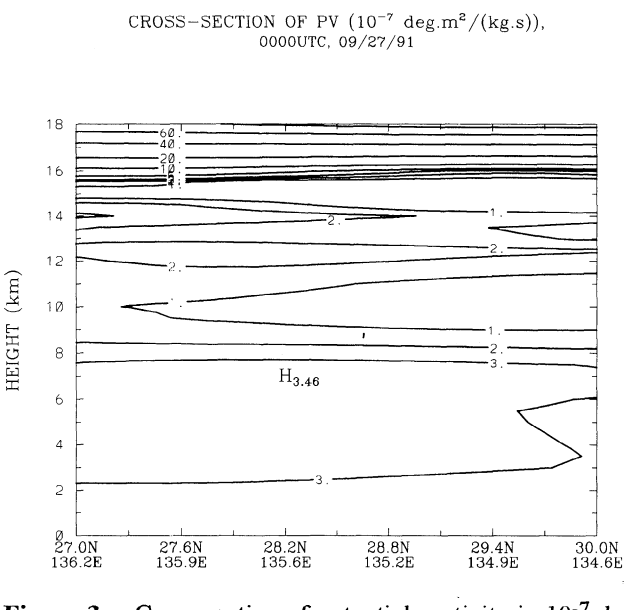


**Figure 3c**. Cross section of potential vorticity in $10^{-7}$ deg $m^2$ $kg^{-1}$ $s^{-1}$ for September 27, 1991. Plate 1 and Figures 3a-3c are in the same plane.

the three high values which appear potentially contaminated, the comparison shows fair agreement between the two techniques with a high bias for MLS at low Lyman-$\alpha$ q values.

## DC-8 Cirrus Versus ECMWF $H_2O$ and Rising Motion

As noted above, aerosols and ozone are measured with DIAL, both above and below the aircraft. The aircraft tracks consist of survey flights from Japan to Hong Kong to Guam to Wake Island to Hawaii and intensive flights with four based in Japan, two in Hong Kong, three in Guam, and one in Hawaii (see *Hoell et al.* [this issue] for details of tracks). The period of sampling was from September 22, 1991, the first intensive flight out of Japan, to October 20, 1991, the only intensive flight out of Hawaii. During this month there were 15 separate flights with cirrus being detected by lidar on 13 out of 14 measurement opportunities (the system could not make cirrus measurements on the flight of October 10). On October 6 no cirrus was observed at all, and this may have been related to the presence of Typhoon Orchid to the southeast. There is often a region of strong subsidence ahead of a typhoon, and this was suggested by the Japanese Geostationary Meteorological Satellite (GMS) images.

On 13 flights the lidar two-dimensional aerosol cross sections suggested that cirrus was present. Similar cross sections of relative humidity and vertical motion were interpolated from the ECMWF grid point data which was available at standard pressure levels of 70, 100, 150, 200, 250, and 300 hPa in the cirrus altitude range; these were spaced about 2 km apart in the vertical. From the lidar profile the latitude, longitude, base, and top of the cirrus were recorded. From the ECMWF profiles the base and top of the layer with greater than 90% relative humidity at the same geographical point was recorded, together with the vertical motion near the center of the lidar layer. For the same cross section used for relative humidity and vertical motion, a cross section of potential vorticity (PV) was drawn up, and its value at the center of the cirrus layer was recorded. An ozone value at the same point was estimated from the DIAL profile.

The parameters described above are shown in Table 2. Also included is an answer to the following question: Was the cirrus near the tropopause as estimated from the DIAL ozone gradient? A summary of the vertical extent of the DIAL image, the extent of almost-saturated air, here defined as greater than 90% relative humidity, and the ECMWF upward or downward motion at the center of the DIAL layer is shown in Figure 2. It can be seen that in 10 cases out of 13 the presence of cirrus in the DIAL results was supported by upward motion and near saturation in the ECMWF data. The three exceptions are October 4 at 21.8°N, where the vertical motion is downward over the cirrus layer; October 13 at 6.9°N, where again there is sinking motion and very little support for cirrus from the relative humidity pattern; and October 20, where at 19.6°N there is scarcely any overlap between the DIAL aerosol and the ECMWF 90% values. To illustrate one of these cases where there is good agreement between the rising motion and the relative humidity, the ECMWF-derived data sets for these two quantities are shown in Figures 3a and 3b, together with the potential vorticity in Figure 3c, for September 27. The DIAL cross section for the same region appears in Plate 1. The typhoon mission, from which this example is derived, is treated elsewhere in this volume [*Newell et al.*, this issue (b)]. Plate 2 and Figures 4a, 4b and 4c give another example of good agreement between the various quantities for October 1. The cirrus cloud forms within the 90% relative humidity centered at 14 and 15.5 km. At 14 km there is rising motion in the ECMWF cross section, though it turns to sinking motion toward the north. Note the very low values of potential vorticity characteristic of the low-latitude troposphere. Plate 3 and Figures 5a, 5b and 5c show the same quantities for October 4. As mentioned above, the vertical motion is downward at 21.8°N, 121°E, but the northern extremity of these profiles at 25.5°N, 122.6°E shows rising motion. This was the worst case of agreement within the sample. Overall, in 10 cases out of 13, there is very good agreement between the analysis of vertical motions and the relative humidity distribution and cirrus cloud observations.

The implication that the aerosol is cirrus cloud rather than stratospheric aerosol is borne out by the characteristics of the images, as noted earlier, and by the fact that the potential vorticity was generally low, in the range from less than 1 to about 6 (in units of $10^{-7}$ deg $m^2$ $kg^{-1}$ $s^{-1}$); for comparison, values of about 15 are often used to delineate the tropopause [e.g., *Hoskins et al.*, 1985]. Ozone is also low in most of those cases, and the cirrus only extended up to the sharp increase in ozone that usually accompanies the tropopause. Considering the relatively small amount of water vapor data that is used as input to the ECMWF analysis (radiosondes plus a limited amount of satellite data), the observed agreement speaks well for the ability of the model to produce the conditions for cirrus clouds, namely, vertical motion and moisture, in regions where they are actually observed by lidar.

## MLS Water Vapor Versus ECMWF Motion Field

Preliminary MLS data at 147 hPa currently have absolute values which are very uncertain, but nevertheless, when averaged for the days available during the PEM-West A mission (September 22 and October 1-20, 1991), they give a coherent pattern shown in Figure 6a. This may be compared with the velocity potentials and associated divergent winds computed for the same period from the ECMWF grid point data (Figure 6b). There is excellent agreement with the position of the moisture maximum seen by MLS and the rising arm of the Walker circulation deduced from ECMWF. At higher levels some of this rising motion may penetrate into the stratosphere, forming what is termed the stratospheric fountain [*Newell and Gould-Stewart*, 1981]. The best season for this penetration is January to February, and its presence will be more evident in the PEM-West B data, when the tropopause and its associated cirrus is higher. Associated with the divergence at 150 hPa, there is a convergence

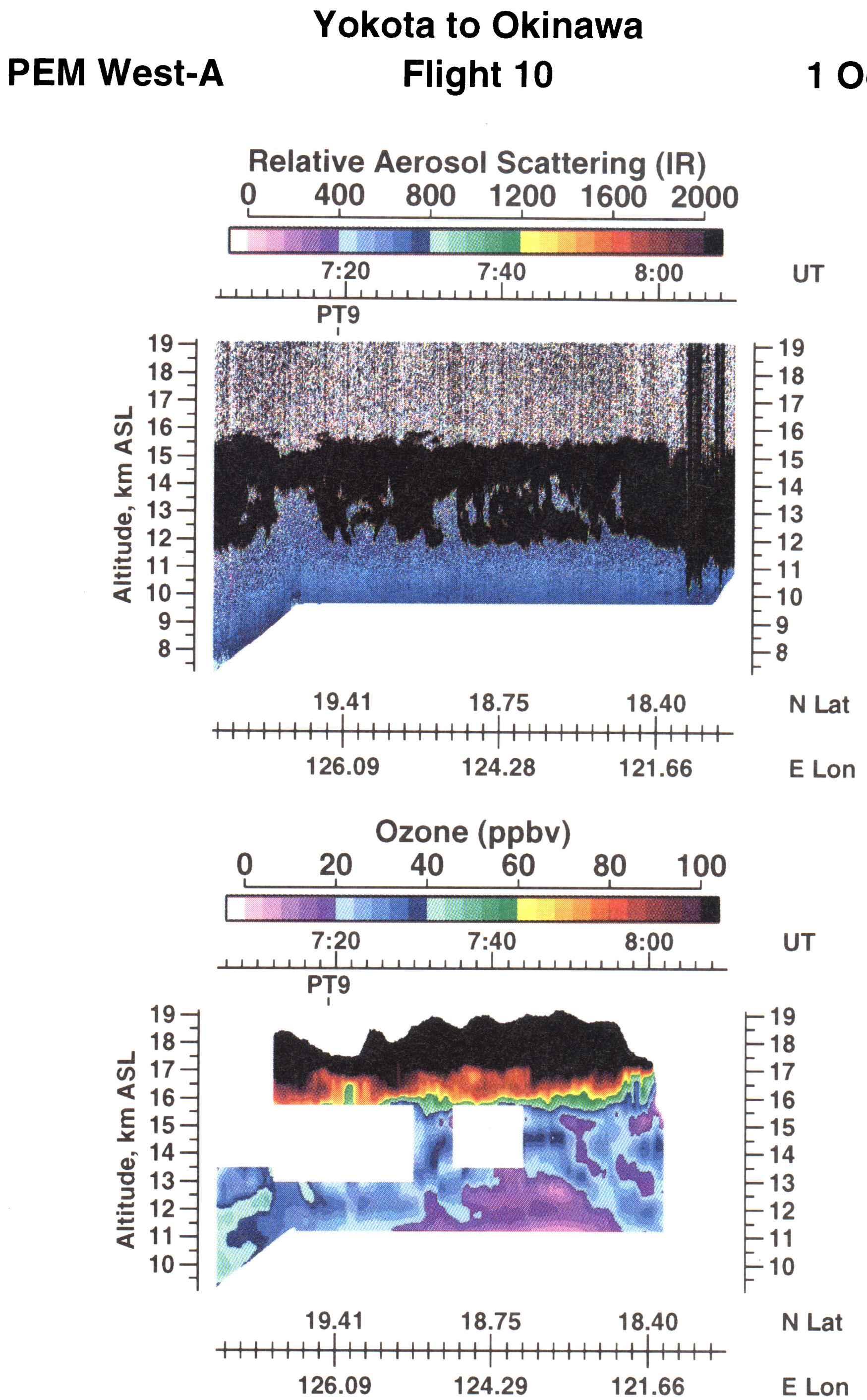


**Plate 2.** DIAL cross section along DC-8 flight track of aerosol and ozone for October 1, 1991.

pattern at 1000 hPa (Figure 6c), which shows that air enters the rising motion regions in the surface layers from a variety of sources, including the continent, the southern hemisphere, and the marine regions to the east. The full set of rotational and irrotational wind components for the PEM-West A period are presented elsewhere in this issue [*Newell et al.*, this issue (a)]. Temperatures at 150 hPa, as analyzed by ECMWF, are shown in Figure 6d. The central column temperature is about -68°C or 205 K, which corresponds to about 15 ppmv of water vapor at saturation over ice, if the constants presented by *Rogers and Yau* [1989, pp. 14-15] are used in the equation for the saturation vapor pressure over ice. This value compares with MLS estimates at the center of the moisture maximum of about 90 ppmv. DIAL-observed cirrus occurrences at or above 14 km (not far from the 147-hPa level) are included in Figure 6a. While cirrus was observed by DIAL at a number of places covered by PEM-West A flights, there was not complete cover. These considerations suggest that the preliminary MLS estimates are biased high at 147 hPa, as expected from the nature of the retrieval algorithm. Over South Korea, where a higher

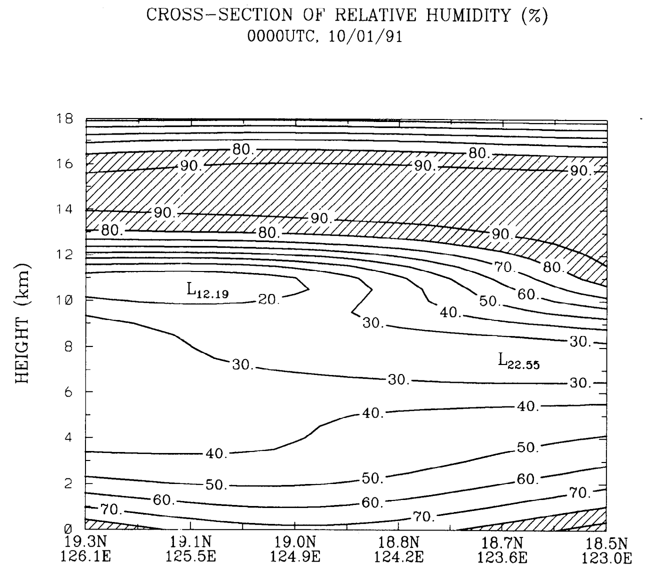


**Figure 4a**. Cross section of relative humidity in percent drawn up from ECMWF grid point data for October 1, 1991. Values >80% shaded.

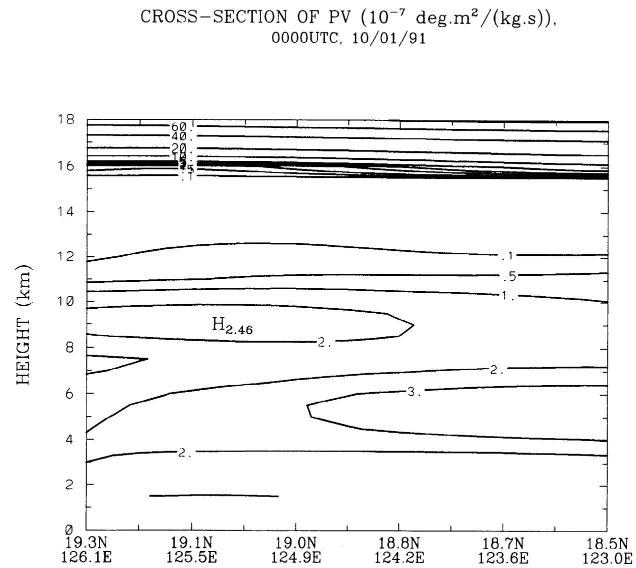


**Figure 4c**. Cross section of potential vorticity in $10^{-7}$ deg $m^2$ $kg^{-1}$ $s^{-1}$ for October 1, 1991. Plate 2 and Figures 4a-4c are in the same plane.

temperature of -58°C occurs, the appropriate saturation mixing ratio is about 60 ppmv, over twice the value observed by MLS, but there are no cirrus data there for comparison.

The situation at 215 hPa (Figure 6e) is somewhat better; MLS mixing ratios at the center of the moisture maximum are about 210 ppmv, while the temperature at 200 hPa is -54°C (not shown) corresponding to a saturation mixing ratio over ice of about 74 ppmv. Again MLS values show a high bias in the moisture maximum. On October 13 the DC-8 was flying at 215 hPa (see Table 1) close to this (mean) central core and its direct measurement of 83 ppmv is in good agreement with the

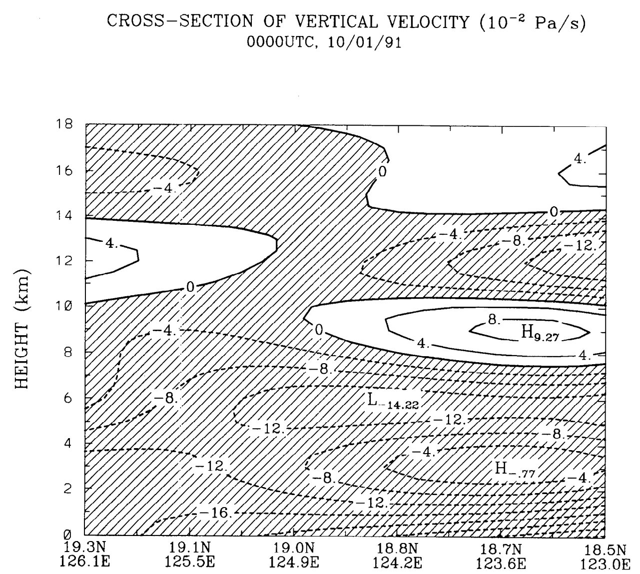


**Figure 4b**. Cross section of vertical motion in $10^{-2}$ Pa $s^{-1}$ from ECMWF data for October 1, 1991. Rising motion shaded.

saturated value reported as haze, which could well have been cirrus. However, over Taiwan the saturation mixing ratio at the observed temperature of -50°C at 200 hPa is 122 ppmv, the same as the MLS value at 215 hPa. DIAL also showed cirrus at this level; the DIAL reports on Figure 6e correspond to cirrus occurring at 12 km.

## Concluding Comments

Comparison of water vapor mixing ratios measured on the DC-8 with a Lyman-α fluorescence instrument with the measurements deduced from MLS at similar heights gives fairly good agreement, with a tendency toward high values by MLS, compared to the Lyman-α measurements, at the low end of the range.

The presence of cirrus derived from the DIAL aerosol cross sections on the DC-8 occurs in 10 cases out of 13 where the ECMWF analyses show rising motion and relative humidity greater than 90%. This agreement between direct observation and values from a model which has little input moisture data at the levels of interest here speaks well for the fidelity of the model.

The mean MLS water vapor pattern at 147 hPa shows a plume centered near 18°N, 145°E, which matches the maximum in velocity potential at the same pressure indicating large-scale rising motion and divergence from that region. Cirrus occurrences from DIAL in the region and this pattern suggest again that the preliminary MLS data may be too high at this pressure level. The situation is better for MLS values at 215 hPa. Though MLS still reads high in the center of the plume, over Taiwan there is a region where DIAL cirrus, MLS, and the saturated mixing ratio appropriate to the ECMWF temperature are all in agreement. It will be of great interest to compare these results with those from PEM-West B carried out in February-March 1994 when the tropopause is higher and

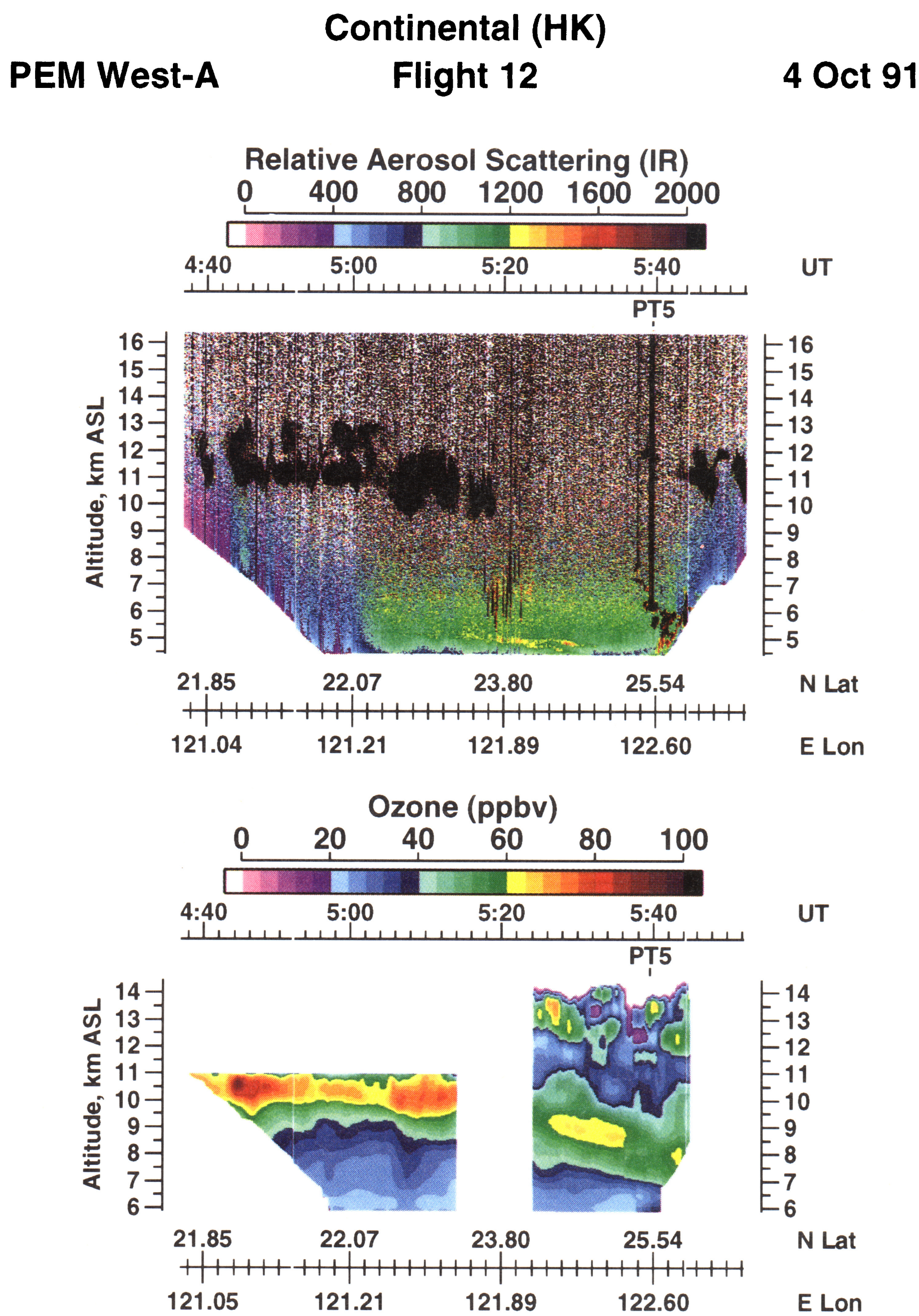


**Plate 3.** DIAL cross section along DC-8 flight track of aerosol and ozone for October 4, 1991.

tropopause temperatures in the West Pacific are near their seasonal lows [*Newell and Gould-Stewart,* 1981].

It is noteworthy that in the early planning of the PEM experiment, much attention was paid to the Walker circulation with its rising arm in the West Pacific and its sinking arm in the East Pacific (these motions being deduced from meteorological data by *Newell et al.* [1974]). It was also known that ozone in the western tropical Pacific upper troposphere, as measured from aircraft, was frequently low, similar to ozone in the tropical boundary layer, and it was suggested that this circumstance was caused by the rising arm of the Walker circulation [*Newell and Wu,* 1985]. In the present study it appears that the rising arm is water vapor rich, consistent with the ozone-poor values found previously. A study of the ozone and water vapor association in layers found by aircraft measurements in situ and ozone layers found from DIAL gives support to these ideas and is discussed elsewhere in this volume.

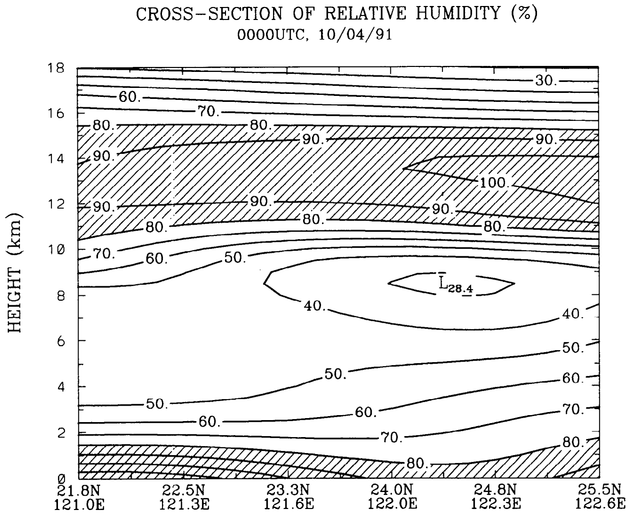


**Figure 5a.** Cross section of relative humidity in percent drawn up from ECMWF grid point data for October 4, 1991. Values >80% shaded.

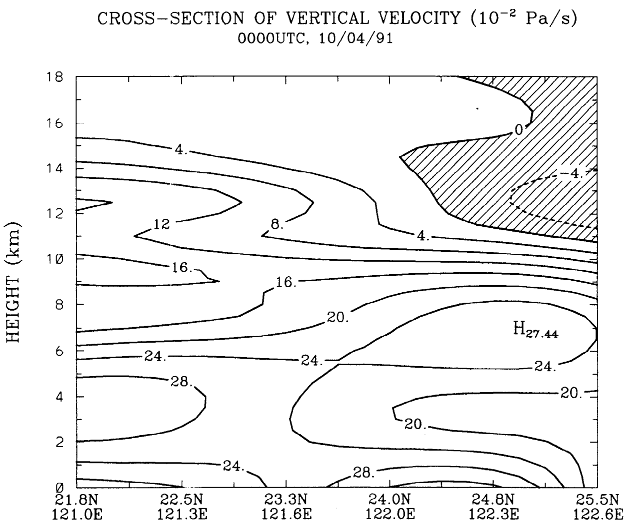


**Figure 5b.** Cross section of vertical motion in $10^{-2}$ Pa $s^{-1}$ from ECMWF data for October 4, 1991. Rising motion shaded.

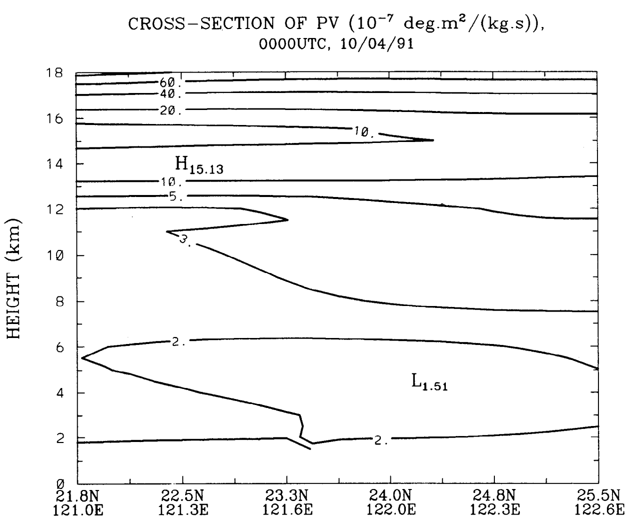


**Figure 5c.** Cross section of potential vorticity in $10^{-7}$ deg $m^2$ $kg^{-1}$ $s^{-1}$ for October 4, 1991. Plate 3 and Figures 5a-5c are in the same plane.

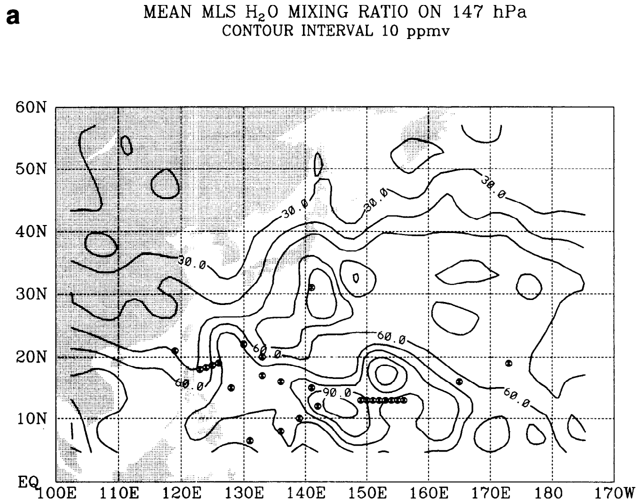


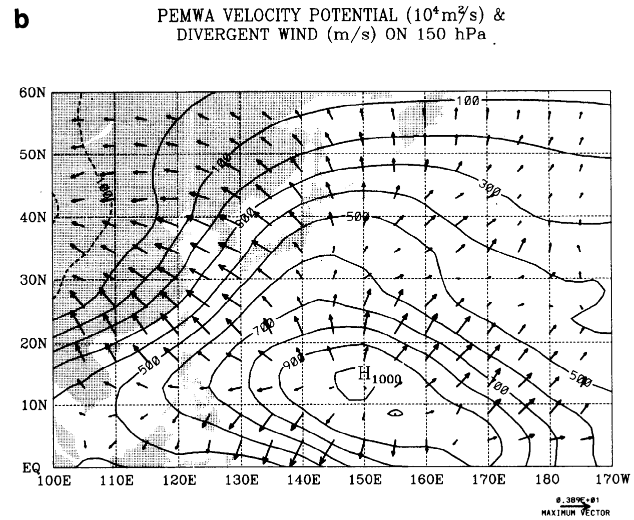


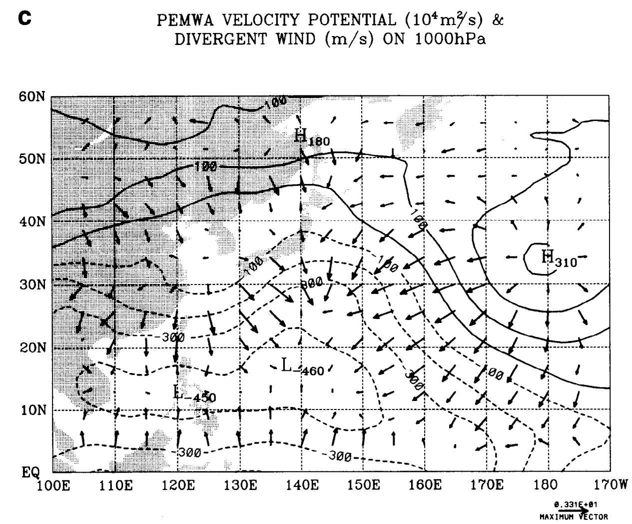


**Figure 6.** (a) Map of MLS water vapor mixing ratio at 147 hPa. Averaged for period October 1-20 and September 22, 1991. Units, parts per million by volume. Contours are for every 10 ppmv. DIAL cirrus occurrences are marked. (b) Mean velocity potential and divergent winds for same period from ECMWF analyses. (c) Same as Figure 6b for 1000 hPa. (d) ECMWF temperature field at 150 hPa. (e) Same as Figure 6a for 215 hPa. Contours are for every 20 ppmv.

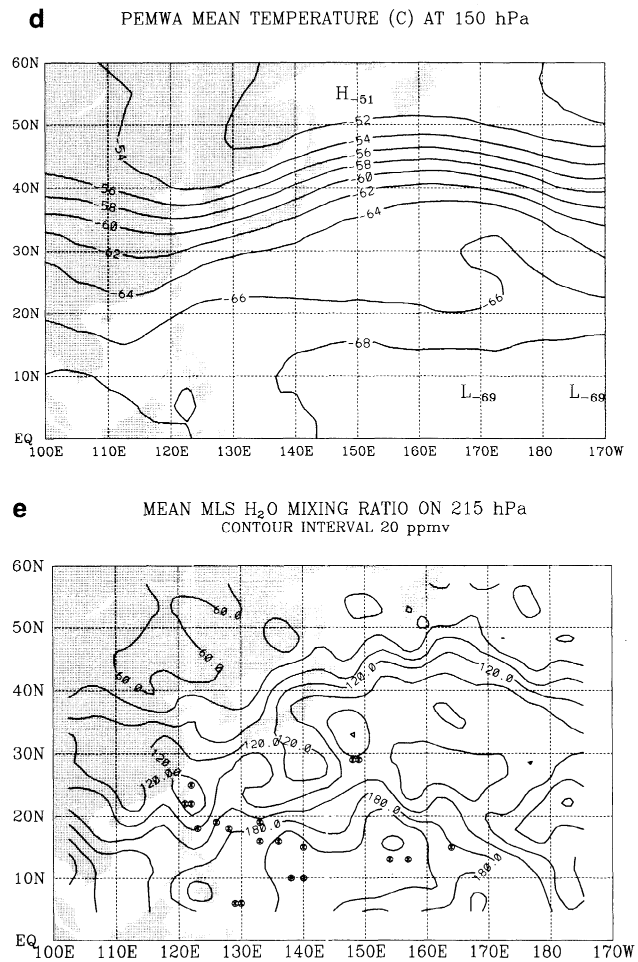


**Figure 6.** (continued)

**Acknowledgements**. Support for this work was provided under the NASA Global Troposphere Experiment, grant NAG-1-1252. The meteorological data were supplied by the European Center for Medium-Range Weather Forecasts.

## References

Barath, F. T., et al., The Upper Atmospheric Research Satellite microwave limb sounder instrument, *J. Geophys. Res., 98*, 10,751-10,762, 1993.

Browell, E.V., et al., Large-scale air mass characteristics observed over the western Pacific during the summertime, *J. Geophys. Res.*, this issue.

Eyre, J. R., G. A. Kelly, A.P. McNally, E. Andersson, and A. Persson, Assimilation of TOVS radiance information through one-dimensional variational analysis, *Q. J. R. Meteorol. Soc., 119*, 1427-1463, 1993.

Hoell, J.M., D.D. Davis, S.C. Liu, R.E. Newell, M.C. Shipham, H. Akimoto, R.J. McNeal, R.J. Bendura, and J.W. Drewry, Pacific Exploratory Mission - West (A) (PEM-West A): September-October 1991, *J. Geophys. Res.*, this issue.

Hoskins, B.J., M.E. McIntyre, and A.W. Robertson, On the use and significance of isentropic potential vorticity maps, *Q. J. Roy. Meteorol. Soc., 111*, 877-946, 1985.

Kelly, K.K., M.H. Proffitt, K.R. Chan, M. Loewenstein, J.R. Podolske, S.E. Strahan, J.C. Wilson, and D. Kley, Water vapor and cloud water measurements over Darwin during the STEP 1987 tropical mission, *J. Geophys. Res., 98*, 8713-8723, 1993.

Kley, D., and E.J. Stone, Measurement of water vapor in the stratosphere by photodissociation with Lyman-$\alpha$ (1216Å) light, *Rev. Sci. Instrum., 49*, 691-697, 1978.

Newell, R.E., J.W. Kidson, D.G. Vincent, and G.J. Boer, *The General Circulation of the Tropical Atmosphere*, vol. 2, pp. 149-178, MIT Press, Cambridge, Mass., 1974.

Newell, R.E., and M.-F. Wu, Simultaneous measurements of carbon monoxide and ozone in the NASA Global Atmospheric Sampling Program (GASP), *Atmospheric Ozone*, edited by C.S. Zerefos and A. Ghazi, pp. 548-552, D. Reidel, Norwell, Mass., 1985.

Newell, R.E., and S. Gould-Stewart, A stratospheric fountain?, *J. Atmos. Sci., 38*, 2789-2796, 1981.

Newell, R.E., Y. Zhu, E.V. Browell, W.G. Read, and J.W. Waters, The Walker circulation and tropical upper tropospheric water vapor, *J. Geophys. Res.*, this issue (a).

Newell, R.E. et al., Atmospheric sampling of supertyphoon Mireille with the NASA DC-8 aircraft on September 27, 1991, during PEM-West A, *J. Geophys. Res.*, this issue (b).

Read, W.G., J.W. Waters, L. Froidevaux, R.F. Jarnot, D.L. Hartmann, R.S. Harwood and R.B. Rood, Upper tropospheric water vapor from UARS MLS, *Bull. Am. Meteorol. Soc.*, 1995.

Rogers, R.R, and M.K. Yau, *A Short Course in Cloud Physics*, 293 pp., Pergamon, Oxford, 1989.

Waters, J.W., Microwave Limb Sounding, chap. 8, in *Atmospheric Remote Sensing of Microwave Radiometry,* edited by M.A. Janssen, pp. 383-496, John Wiley, New York, 1993.

E. V. Browell and S. Ismail, NASA Langley Research Center, Mail Stop 401A, Hampton, VA 23681-0001. (e-mail: e.v. browell@larc.nasa.gov)

K. K. Kelly and S. C. Liu, NOAA Aeronomy Laboratory, R/E/AL-4, 325 Broadway, Boulder, CO 80303.

R. E. Newell (corresponding author) and Y. Zhu, Department of Earth, Atmospheric and Planetary Sciences, Massachusetts Institute of Technology, 77 Massachusetts Avenue, Room 54-1824, Cambridge, MA 02139. (e-mail: newell@newell1.mit.edu; zhu@newell1.mit.edu)

W. G. Read and J. W. Waters, Jet Propulsion Laboratory, Mail Stop 183-701, 4800 Oak Grove Drive, Pasadena, CA, 91109.

(Received July 20, 1994; revised March 19, 1995; accepted March 30, 1995.)